AGU PUBLICATIONS

Geophysical Research Letters

RESEARCH LETTER

10.1002/2015GL063877

Key Points:
- Shifts in total rainfall amount primarily drive rainfall-related crop yield change
- Increased rainfall intensity improves dryland crop yields more than frequency
- A delayed rainy season onset, in general, leads to yield loss in West Africa

Supporting Information:
- Text S1 and Figures S1–S10

Correspondence to:
K. Guan, and B. Sultan,
kaiyug@stanford.edu;
Benjamin.sultan@locean-ipsl.upmc.fr

Citation:
Guan, K., B. Sultan, M. Biasutti, C. Baron, and D. B. Lobell (2015), What aspects of future rainfall changes matter for crop yields in West Africa?, *Geophys. Res. Lett.*, *42*, doi:10.1002/2015GL063877.

Received 16 MAR 2015
Accepted 17 SEP 2015
Accepted article online 23 SEP 2015

©2015. The Authors.
This is an open access article under the terms of the Creative Commons Attribution-NonCommercial-NoDerivs License, which permits use and distribution in any medium, provided the original work is properly cited, the use is non-commercial and no modifications or adaptations are made.

What aspects of future rainfall changes matter for crop yields in West Africa?

Kaiyu Guan[1], Benjamin Sultan[2], Michela Biasutti[3], Christian Baron[4], and David B. Lobell[1]

[1]Department of Earth System Science and Center on Food Security and the Environment, Stanford University, Stanford, California, USA, [2]Sorbonne Universités (UPMC, University of Paris 06)-CNRS-IRD-MNHN, LOCEAN/IPSL, Paris, France, [3]Lamont-Doherty Earth Observatory, Earth Institute at Columbia University, Palisades, New York, USA, [4]CIRAD UMR TETIS, Maison de la Télédétection, Montpellier, France

Abstract How rainfall arrives, in terms of its frequency, intensity, the timing and duration of rainy season, may have a large influence on rainfed agriculture. However, a thorough assessment of these effects is largely missing. This study combines a new synthetic rainfall model and two independently validated crop models (APSIM and SARRA-H) to assess sorghum yield response to possible shifts in seasonal rainfall characteristics in West Africa. We find that shifts in total rainfall amount primarily drive the rainfall-related crop yield change, with less relevance to intraseasonal rainfall features. However, dry regions (total annual rainfall below 500 mm/yr) have a high sensitivity to rainfall frequency and intensity, and more intense rainfall events have greater benefits for crop yield than more frequent rainfall. Delayed monsoon onset may negatively impact yields. Our study implies that future changes in seasonal rainfall characteristics should be considered in designing specific crop adaptations in West Africa.

1. Introduction

Theory and modeling studies have suggested that the West Africa monsoon region will experience complex and regional-dependent changes in intraseasonal rainfall characteristics under a warming climate [*Monerie et al.*, 2012; *Biasutti*, 2013]. Long-term observations already depict robust trends in rainfall frequency and intensity, with many parts of Sahel showing a decreased number of rainy days and an increase in rainfall intensity and extreme heavy rainfall events [*Lodoun et al.*, 2013; *Panthou et al.*, 2014]. While it is well known that intraseasonal rainfall characteristics, such as long dry spells after sowing [*Sivakumar*, 1992], can be important for yield in this region where more than 95% of all the agriculture is rainfed, it remains unclear whether the specific rainfall changes projected for the next few decades will exert large effects on the major crops of the region.

Understanding crop responses to possible shifts in intraseasonal rainfall patterns is useful for at least three reasons. First, when designing crop modeling studies to assess impacts of climate changes, it is important to know which aspects of rainfall are essential to include for agricultural planning. For example, previous studies commonly use only changes in seasonal or annual aggregated total rainfall [e.g., *Sultan et al.*, 2013], a simplification that can facilitate more rapid assessments with multiple crop models [e.g., *Ruane et al.*, 2014] but may miss some critical impacts associated with, for instance, intraseasonal dry spells. Second, if certain aspects of rainfall are particularly important to crops, this knowledge can inform the design of adaptation strategies within agriculture. For example, if increased intensity is especially damaging, adaptations might focus on rainwater harvesting. Third, if the intensity, frequency, and/or seasonality of rainfall are important for crops, this knowledge could help prioritize climate research needs toward reducing uncertainties in simulating those aspects that are most relevant.

The idea that intraseasonal rainfall characteristics are important for crop modeling is not new, but previous work mostly focused on how the errors in these rainfall features in climate data sets propagate into crop simulations. Typical gridded climate data, from satellite retrievals, reanalysis, or climate model outputs, usually suffer from too much drizzle and a large bias in rainfall frequency (up to 100%) [*Baron et al.*, 2005; *Berg et al.*, 2010; *Ramarohetra et al.*, 2013], which can subsequently bias simulated crop yield. Though the absolute magnitudes of rainfall characteristics simulated by climate models may have their biases [*Crétat et al.*, 2013], the simulated relative change in intraseasonal rainfall characteristics under various climate change scenarios could be more reliable and indeed it is our best guidance for projecting future changes [*Glotter et al.*, 2014]. The projected changes of intraseasonal rainfall characteristics in Africa from historical

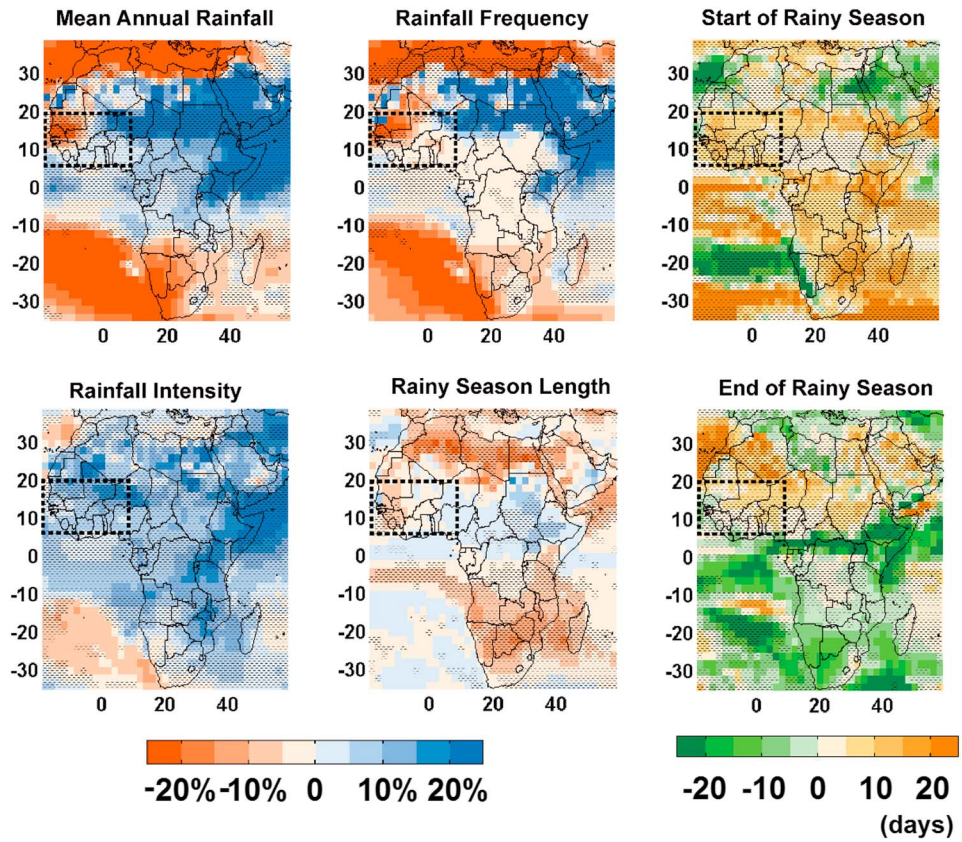

Figure 1. Projected changes of rainfall patterns (mean annual rainfall, rainy-season rainfall frequency, rainy-season rainfall intensity, rainy season length, and start and end of rainy season) from 16 models of CMIP5, as the difference of 2061–2090 (RCP8.5 scenario) minus 1961–1990. The blue/red color shades refer to the changes relative to the historical period (1961–1990); the green/brown color shades refer to absolute changes in days. Meshed regions indicate that 70% of the models show the same direction of changes. The dashed black box indicates the targeted region in this study.

and RCP8.5 scenario simulations from 16 models (see Appendix A) from the Coupled Model Intercomparison Project 5 (CMIP5) [*Taylor et al*., 2012a] are shown in Figure 1. We adopt the approach detailed in section 2.3 (also see the supporting information for how to derive "rainy season length") to analyze projected changes in rainfall characteristics between the periods 1961–1990 and 2061–2090 (individual model patterns can be found in Figure S10 in the supporting information). Focusing on West Africa (box in Figure 1), we have the following findings: (i) an overall rainy season delay in the whole region (significant delay in both start and end of rainy season and insignificant changes in total rainy season length; "significant" means that 70% of all the models show the same sign of changes), consistent with previous findings [*Biasutti and Sobel*, 2009; *Biasutti*, 2013]; (ii) an overall increase in rainfall intensity (0–15%) and an overall decrease of rainfall frequency (−5%−20%) across nearly the whole region; and (iii) a dipole pattern in the projected mean annual precipitation (MAP) change; i.e., the east part of West Africa has an increase in MAP attributing to a large increase in rainfall intensity as well as a slight increase of rainy season length, and the west part of West Africa exhibits decreased MAP mostly due to the decrease of rainfall frequency.

In this paper, we design a new stochastic rainfall model to synthetically generate different rainfall change scenarios that are relevant to the projected rainfall changes in CMIP5 (Figure 1) at the 35 stations spanning West Africa. We then use these synthetic climate variables to drive two regionally calibrated and validated crop models to understand how different aspects of intraseasonal rainfall variability affect the yield of sorghum, one of the main staple crops in the Sudanian and Sahelian savannas of West Africa. We employ two crop models to reduce the model-dependent uncertainty and increase the robustness of the simulation results. To separate rainfall effects from other important factors, we use the historical-level temperatures and atmospheric CO_2 concentrations. Our results are not sensitive to this choice: we conducted additional simulations, using a higher

temperature (e.g., +2°C) or higher CO_2 concentrations (up to 530 ppm) to mimic the near-term (i.e., the next 20–50 years) climate change scenarios, and found no qualitative changes in results (Figure S9). This assures that the interactions between the changes of intraseasonal rainfall characteristics and temperature or CO_2 concentrations have little impact on our conclusions related to yield responses to intraseasonal rainfall characteristics. We also assess the responses of two sorghum cultivars, representing traditional and modern types which mainly differ in their photoperiod sensitivity (thus the growing length) and potential yields [*Sultan et al*., 2014].

2. Methods

2.1. Study Area and Meteorological Station Data

Our study area covers West Africa, which is an important food production area in Africa, spanning from 18°W to 5°W in longitude and 10°N to 18°N in latitude (highlighted in dashed black box in Figure 1). We focus on 35 sites where daily meteorological observations have been compiled by the AGRHYMET Regional Center and National Meteorological Agencies for the 1961–1990 period. Daily rainfall, solar radiation, surface wind speed, humidity, and temperature were measured. These 35 sites span the whole region and cover a wide range of annual total rainfall from 250 mm/yr to 2100 mm/yr (Figure S1).

2.2. Two Crop Models and Two Major Cultivars

We employ two different crop models in this study to simulate sorghum yields: SARRA-H (version 3.2) [*Kouressy et al*., 2008] and APSIM (version 7.5) [*Hammer et al*., 2010], both of which have been calibrated with the same field trial data [*Dingkuhn et al*., 2008; *Traoré et al*., 2011] and have been tested against regional crop statistics [*Sultan et al*., 2014]. Both models incorporate processes of soil water balance, plant carbon assimilation, and biomass partitioning. One major distinction between the two crop models is that APSIM can simulate nitrogen stress on crop production. Though both models include mechanisms to simulate photoperiod sensitivity of crop growth, their approaches differ [*Dingkuhn et al*., 2008; *Kumar et al*., 2009], which may induce different responses to the shifts of rainy season. Detailed overviews of the two models and a description of soil parameters used can be found in *Sultan et al*. [2014].

Because the importance of intraseasonal rainfall characteristics could vary depending on the growth patterns of different crop cultivars, we simulate two well-known local sorghum cultivars in our study. The traditional cultivar has moderate to strong photoperiod sensitivity [*Kouressy et al*., 2008] and a longer crop cycle length (~150 days from sowing to maturity) but smaller average yields. The modern cultivar is an early-maturing, short-duration (~95 days from sowing to maturity), and photoperiod-insensitive crop selected to maximize the mean yield under optimal fertility conditions. On-farm surveys in West Africa [*Traoré et al*., 2011] indicate that a large majority of farmers in West African countries use the traditional cultivar, with a small fraction of farmers having adopted the modern cultivar.

2.3. Stochastic Rainfall Model and Weather Generator

To quantify crop yield responses to seasonal rainfall variability, we first design a new stochastic rainfall model based on *Guan et al*. [2014a] but adding explicit time-varying parameters of rainfall frequency and rainfall intensity, which implicitly include the phase and length information of rainy season. In the approach of *Guan et al*. [2014a], a daily rainfall time series for a continuous period is simulated as a marked Poisson process [*Rodriguez-Iturbe et al*., 1999]. The arrival of rainfall events is a Poisson process; i.e., the distribution of time t between rainfall events is exponential with mean $1/\lambda$, and λ is estimated as the mean of rainfall frequency (events/day): $f_t(\tau) = \lambda e^{-\lambda\tau}$, for $\tau \geq 0$ (with τ as dummy variable). The depth of rainfall events is exponentially distributed with mean α, and α is estimated as the mean of rainfall depth only from the rainy days (mm/event): $f_H(h) = \frac{1}{\alpha} e^{-\frac{1}{\alpha}h}$, for $h \geq 0$ (with h as the dummy variable). A rainy day is defined when total daily rainfall is more than 0 mm/d, and we consider one rainy day as one rainfall event (i.e., there is no consideration of subdaily rainfall events, which is consistent with the time step of crop model input). Thus, the cumulative total rainfall for a certain period τ_i has the mean of $\lambda_i \alpha_i \tau_i$ (mm), with subscript i referring to a specific period.

To capture seasonal variations in both rainfall frequency and intensity, we estimate λ and α for each day of the year (DOY, DOY = 1–365) centered at a moving window of 21 days (10 days at each side) from the whole historical rainfall periods. That is, we join all rainfall records within this DOY window period and treat the

newly formed rainfall sequence as a statistically homogeneous time series, from which we estimate the corresponding λ and α for this DOY period. Figure S2 shows an example of derived rainfall frequency and intensity from a 30 year daily rainfall record from a site in West Africa. Based on the above definition, we do not need to explicitly estimate rainy season length, as the time-varying rainfall frequency and intensity have implicitly included the seasonal magnitude and phase information.

We then use the mean of the estimated daily λ and α for this period (here 20 days as an interval) to represent the aggregated rainfall characteristics and use the marked Poisson process to generate synthetic rainfall time series. We repeat this step for each 20 day interval from the first day to the last day of the year. Our rainfall model can well capture both the total amount (slope = 0.99, $R^2 = 0.997$, $p < 10^{-5}$) and seasonal variation (slope = 0.82, $R^2 = 0.975$, $p < 10^{-5}$) for rainy seasons across the 35 sites in our study area (Figure S3). We focus on the seasonal-scale rainfall rather than interannual variation, as the focus of this study is related to crop yield response to intraseasonal rainfall variation. It is worth noting that our rainfall model has a light underestimation in seasonal variation, mostly due to the assumption of stochastic distribution of rainfall intensity. We chose an exponential distribution here [*Rodriguez-Iturbe et al*., 1999], which may not be able to simulate very heavy rainfall events (due to the thin tail of exponential distribution). Using more heavy-tail distributions can solve this issue, though we do not expect a significant difference in our results, as the current approach captures the majority (82%) of the rainy season rainfall variability.

Uncertainties of estimated λ are small (<5%) and well constrained across the whole year (Figure S2). Uncertainties of estimated α are small during the rainy season and only become large during dry season due to too few samples in these periods. We thus force dry season α to be zero (the "dry season" is defined in the supporting information).

The setup of our rainfall model makes it easy to manipulate intraseasonal rainfall characteristics. Rainfall frequency or intensity changes are realized by multiplying the baseline values with a scaling factor. To change rainy season length, we first derive the center of the rainy season based on the concept of *Markham* [1970] (see supporting information) and then proportionally extend or shrink the baseline rainfall frequency and intensity from the center of rainy season to the two ends of the rainy season. After the extension (e.g., 1 year rainfall record after 10% extension in length would yield a time series of $365 \times 1.1 = 402$ days), we simply truncate these parts that exceed the length of a year at the two sides. Similarly, after a shrinkage, we fill zero values on both sides, assuming that the dry season has no rainfall events. By doing so, we are able to lengthen or shorten the rainy season length and meanwhile preserve the seasonal pattern of rainfall frequency and intensity. To shift the rainy season (e.g., delay or advance), we move the rainfall frequency and intensity forward or backward and do the same truncation and zero filling as before.

After generating the rainfall time series, to preserve the covariance between rainfall and other climate variables, we conditionally resample other climate variables from the historical climate record. In particular, for a specific DOY, we search the historical record within 10 days of the targeted DOY and look for the date whose rainfall record best matches the synthetic rainfall amount in terms of the smallest absolute difference. If there is more than one suitable sample in the historical pool, we randomly choose one. Then we take all climate variables except rainfall of that chosen day to complete the synthetic weather record. To further account for the uncertainties arising from our stochastic rainfall model and the weather resampling approach, we also generate multiple realizations of rainfall and the corresponding climate forcing for each specific type of rainfall change (see details in section 2.4).

The simulated crop yields from both APSIM and SARRA-H forced by historical climate observation and forced by our synthetically generated climate based on the derived historical rainfall characteristics are highly consistent (Figure S4). The latter simulation is also called the "baseline" run.

2.4. Experiments Design and Implementation

Based on the projected rainfall changes (Figure 1), we design the three following experiments using the framework of our stochastic rainfall model (i.e., seasonal total rainfall = $\lambda \times \alpha \times \tau$, where λ is rainfall frequency, α is rainfall intensity, and τ is rainy season length):

Experiment (1): Total annual rainfall changed by ±10%, by varying only one of the three rainfall characteristics (i.e., λ_i, α_i, or τ_i).

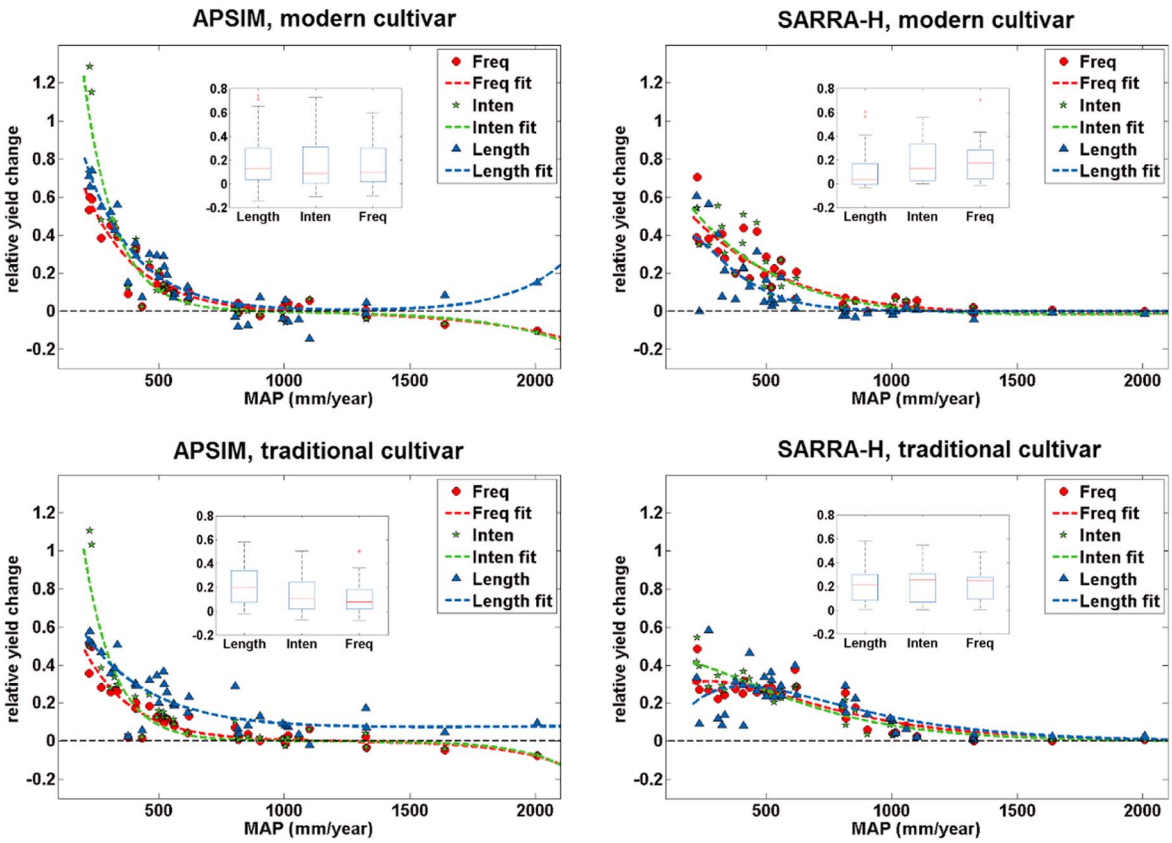

Figure 2. Relative yield change (normalized by the simulated yield in the baseline runs) to the change in total annual rainfall ([+10%] − [−10%], Experiment (1)), which is realized through the changes in rainfall frequency, rainfall intensity, and rainy season length. Each point corresponds to the results from a station. The *y* axis means that if there is a 1% change in total rainfall, it would lead to 1% × relative yield change (*y* axis value) of the crop yield. The dashed lines are the robust Lowess fits for the results. The insets show the averaged pattern of all 35 sites for the three scenarios, with median (red line) and 25% and 75% quantiles (as the lower and upper bounds) indicated.

Experiment (2): We fix total annual rainfall but vary ±30% of rainfall frequency with corresponding change in rainfall intensity to keep the total annual rainfall the same.
Experiment (3): Without changing total annual rainfall, we delay the phase of rainy season by 10% of its original season length.

Experiment (1) mainly tests whether crop yields are sensitive to different realizations for the same change in total annual rainfall amount. The range of change used in Experiment (1) (i.e., ±10%) is based on the ensemble projections from the CMIP5 models (Figure 1). Experiment (2) further studies the relative importance of rainfall frequency and intensity change under a fixed annual rainfall total. We choose ±30% of rainfall frequency because this is the upper bound of future climate projections (Figure 1), and such variations in rainfall intensity have also been observed in the study region during the period of 1970 to 2000 [*Lodoun et al.*, 2013]. We also checked the results of only varying ±10% or ±20%, and we find similar patterns but with smaller magnitude. Experiment (3) addresses yield responses to rainy season delays of a magnitude which is anticipated in West Africa (Figure 1).

Since the synthetic weather generator is based on a stochastic process, for each simulation we generate 15 ensembles to drive two crop models and use the ensemble mean of crop-simulated yields for the analysis. The ensemble number is set as 15 as more ensembles start to reach a plateau in marginal benefit (Figure S5). Two models have similar sowing rules, and both are based on the rainfall amount and soil moisture status at the beginning of the rainy season [*Sultan et al.*, 2014]. Thus, sowing date mostly follows the trend of rainy season onset. We fix the atmospheric CO_2 concentration to be 350 ppm for all the simulations. For APSIM we only show the results with a fertilizer rate of 50 kg/ha. Simulations with a low fertilizer rate of 10 kg/ha show very similar responses to changes in rainfall characteristics.

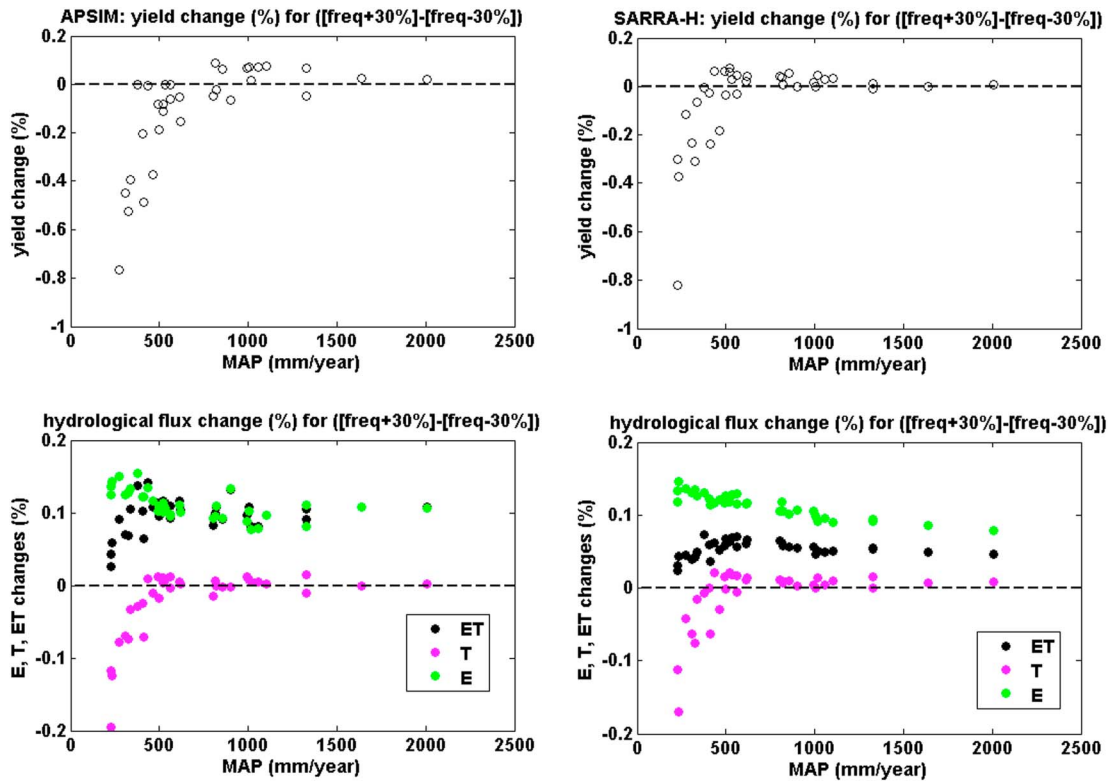

Figure 3. (top row) Simulated relative yield change of higher-frequency case (+30%) minus lower frequency case (−30%) (i.e., Experiment (2)), normalized by the baseline yield in APSIM and SARRA-H, as a function of MAP. (bottom row) The difference of hydrological fluxes for the same experiment in two models, normalized by the baseline ET value.

3. Results

The results of Experiment (1) reveal that crop yield response to a change in MAP is primarily a function of the baseline total annual rainfall, with relatively small sensitivity to what rainfall characteristic was changed to achieve the MAP change (Figure 2). Both crop models show consistent patterns: simulated yields respond alike to the same percentage change in rainfall frequency, rainfall intensity, and rainy season length for a given cultivar. The yield-MAP fitted curves by robust Lowess fits for the three rainfall characteristics have a similar trend: simulated yields have larger relative change at low MAP and become less sensitive at higher MAP. It is worth noting that the patterns shown in Figure 1 is 1~4 times larger than the uncertainties of the ensemble simulation for baseline condition (Figure S6), meaning that the detected signal is robust.

Although responses to changes in the three rainfall characteristics are broadly similar, some differences are apparent at both high and low MAP. At very high MAP (>1500 mm), APSIM yields decrease with higher frequency or intensity, though SARRA-H shows little yield response. This unique response of APSIM is related to its nitrogen sensitivity, which is not considered in SARRA-H. At high MAP, additional rainfall increases nitrogen leaching and results in elevated nitrogen stress. APSIM captures this response in its measure of the ratio of nitrogen supply to plant demand ("nitrogenSD"), which increases by ~30% for the two highest MAP sites at a higher frequency or intensity case.

At low MAP, both models indicate that yields benefit more from increases in intensity than in frequency or rainy season length (Figure 2). This is confirmed in Experiment (2), where we fix the MAP but vary rainfall frequency and intensity simultaneously (Figure 3, top row). At low MAP (below ~600 mm/yr in APSIM or below ~500 mm/yr in SARRA-H), corresponding to the semiarid conditions of the northern Sahel, higher rainfall frequency leads to a lower crop yield (−80%–0%). This negative difference becomes smaller with increased MAP, and beyond 600 mm/yr in APSIM (or 500 mm/yr in SARRA-H), higher frequency starts to have comparable or slightly better effects than the same percentage increase in intensity.

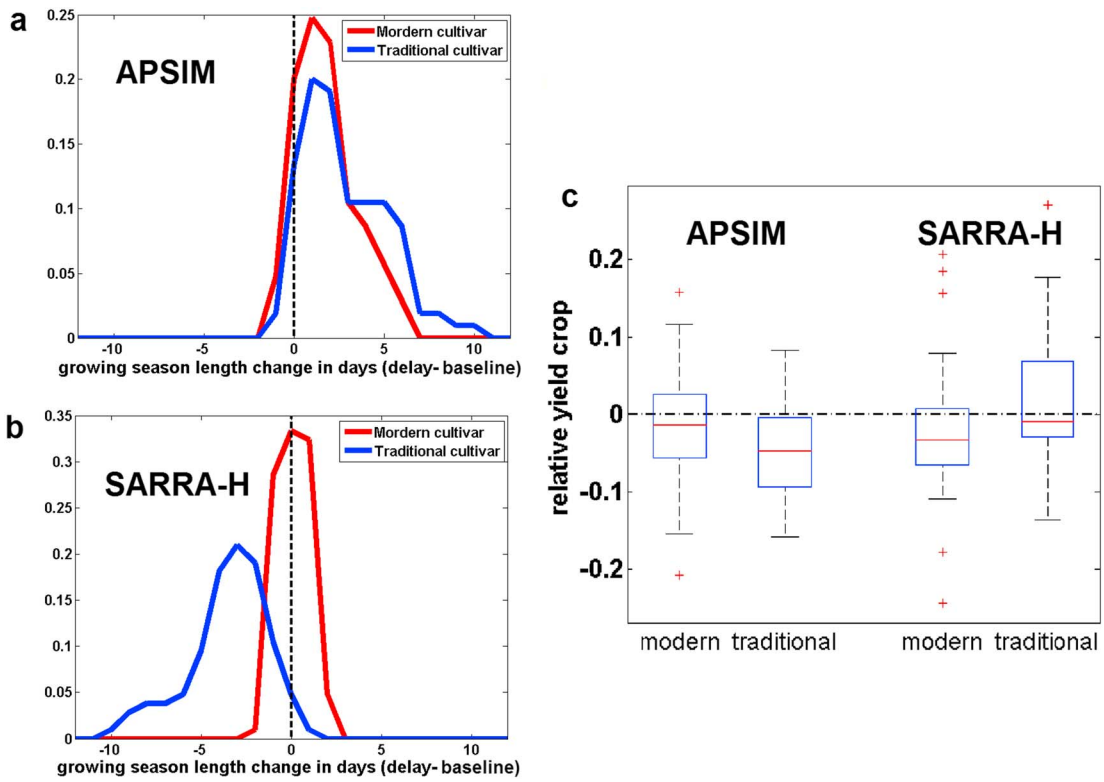

Figure 4. (a and b) Growing season length change for Experiment (3), i.e., 10% delay of rainy season − baseline run, and (c) corresponding yield change in two models and two cultivars.

The above results can be largely explained by the simulated hydrological fluxes from the two models (Figure 3, bottom row). With increased rainfall frequency and correspondingly reduced intensity (i.e., Experiment (2)), simulated evapotranspiration (ET) increases overall because of reduced runoff. However, at low MAP, it is only the evaporation (*E*, from both canopy interception and shallow soil moisture) that increases, reducing soil moisture supply that can be used by crops. Crop transpiration (T) is reduced accordingly, limiting plant photosynthesis and growth. Thus, higher frequency (and meanwhile lower intensity) of rainfall reduces yield when MAP is below 600 mm/yr in APSIM (below 500 mm/yr for SARRA-H).

Differences between the responses of traditional and modern cultivars are similar across both models. For all but the lowest MAP, the traditional cultivars have higher yield increases under the same increase of rainy season length than the modern cultivar (blue points and lines in Figure 2). Under an increased rainy season length (i.e., advanced onset and delayed end of rainy season), both cultivars are sown earlier in the models. However, the modern cultivar has a short growth cycle and weak photoperiod sensitivity; thus, it correspondingly matures earlier, leading to an overall advanced growing cycle with little change in its total growth length. In contrast, the traditional photoperiod-sensitive cultivar matures at the similar time as before and have a longer growth cycle, and thus can better take the advantage of the increased rainy season length and increased total rainfall amount.

Finally, we focus on the yield response to a delayed rainy season (10% of the rainy season length at each site, Experiment (3)). The consistent pattern is that both models show a yield decrease in this scenario. Meanwhile, two models simulate different sensitivities between cultivars: in APSIM, traditional cultivars are the worst affected, while in SARRA-H the modern cultivars show the largest decrease in yield. These distinct behaviors are due to differences in the model parameterization of sorghum's photoperiod sensitivity. Sorghum is a short-day plant; i.e., it develops more rapidly on short days [*Major*, 1980], and this photoperiod sensitivity usually occurs prior to floral initiation [*Alagarswamy et al.*, 1998]. APSIM adopts a linear relationship between plant thermal requirements (i.e., growing degree day, GDD) and day length [*Kumar et al.*, 2009] and uses field phenology observation to calibrate the parameters. A delayed rainy season leads to a corresponding delay in sowing and thus also, for all early-sowing sites, shift the plant's growth period into a time of year with longer days (Figure S7). This causes an increase of the GDD thermal requirement and a lengthening of the growth

cycle. The growth of traditional cultivars lengthens the most, due to a stronger photoperiod sensitivity (simulated as a larger slope for the GDD-day length relationship). The longer growth cycle generally causes a yield loss in APSIM, mostly because a further extension of the growth cycle may lead to more water stress for the plants that are still growing after the end of the rainy season. This is illustrated by the simulated water stress ("waterSD," Figure S8), which is highly correlated with the yield changes in APSIM. SARRA-H adopts a more complex algorithm to parameterize the photoperiod sensitivity, which includes both the day length and the crop's existing thermal history, yet the parameterization depends on calibration to existing varieties [*Dingkuhn et al*., 2008]. In our hypothetical scenario of a delayed rainy season, APSIM dynamically adapts to different regions by changing the latitude-dependent day length, while SARRA-H has no appropriate data to calibrate the effects of different day lengths. Thus, SARRA-H simulates smaller variations in growing length in links with latitude change, i.e., a nearly fixed maturity date for all sites in the current study. Therefore, in SARRA-H, a delayed rainy season for the traditional cultivar would not change the total rainfall that crops receive during their growing cycle (the harvest time in SARRA-H is usually later than the end of rainy season), which leads to little change in yield (Figure 4b). The reason for a yield loss of modern varieties under a delayed rainy season remains less clear, and it is less relevant due to the limited calibration in SARRA-H for the scenario of a delayed rainy season. Given the difference between the cultivars in two models, it is worth emphasizing a robust pattern: across all these situations, yield loss happens after a delay of rainy season.

4. Discussion

Our results from Experiment (1) generally provide a justification for focusing on seasonal total rainfall as a first-order predictor to assess rainfall impacts on yields. Simulations from both crop models confirm that different intraseasonal rainfall characteristics, within a plausible range based on climate model projections, have relatively smaller impacts. This contrasts somewhat with the reported large impacts of rainfall frequency by *Berg et al*. [2010], which compared simulations using raw gridded daily climate products versus data that had been corrected to have realistic rainfall frequencies. The main distinction is that our experiment varies rainfall frequency over a relatively narrow range intended to be consistent with future climate projections (±10% change of the climatological range), whereas *Berg et al*. [2010] varied rainfall frequency up to 100%. Thus, although it is important to not have completely unrealistic rainfall frequencies (as many climate model simulations have), fairly small changes over the next few decades are unlikely to matter much, except at the very dry sites (with MAP below 500–600 mm/yr, which is discussed below).

One unexpected result from Experiment (1) is that crops have a much smaller response in yield to an increased rainy season length than natural savanna ecosystems [*Guan et al*., 2014a, 2014b]. This difference mainly arises from different phenological controls between natural grasslands and crops. The growing period of the former is mostly determined by rainy season; thus, a lengthening of the rainy season translates to a longer growing season and higher productivity. Instead, the phenology of crops follows accumulative thermal conditions and photoperiods, and their growing length has less dependency on the rainy season length. This finding may also have some important implications for other dryland agriculture, such as those in the southern part of the African continent, where future climate projections show a robust rainy season shortening (Figure 1). Whether those drylands have similar responses to the rainy season length change is worth further investigation but is beyond the scope of the current study.

Despite the first-order importance of aggregated rainfall amount, our study from Experiment (2) identifies a secondary importance of rainfall frequency and intensity at MAP below 600 mm/yr (for APSIM and 500 mm/yr for SARRA-H). More frequent rainy days were traditionally thought to be beneficial for plant growth [e.g., *Good and Caylor*, 2011]. However, in West Africa, low MAP usually corresponds to low rainfall frequency [*Guan et al*., 2014a]. Both crop models simulate runoff based on the saturation-excess mechanism, which essentially treats the soil column as a bucket: when the water storage capacity of the soil is met, runoff ensues. This approximation is reasonable considering that the infiltration-excess mechanism for runoff can be ignored at the daily timescale that is used for both crop models. Our results show that further increasing frequency at low MAP leads to less penetration of rainfall into deep soil layers and more evaporation from both shallow soil layer and canopy interception, thus reducing the available soil moisture for plant water use and causing crop yield loss. Therefore, the benefits of reduced runoff are apparently outweighed by the costs of higher evaporation. The benefits of more frequent rainfall only emerge when MAP is larger than

600 mm/yr (for APSIM and 500 mm/yr for SARRA-H) in our study, consistent with many previous findings [*Thomey et al*., 2011; *Guan et al*., 2014a]; by then the increased rainfall frequency would effectively reduce the intervals between low soil moisture states, thus reducing plant water stress [*Porporato et al*., 2004]. We thus conclude that the projected increase of rainfall intensity in West Africa (Figure 1) has a potential benefit for crop yields at drier sites. It is worth noting that our results are dependent on the model structure. In particular, the two crop models only simulate saturation-excess runoff at the daily scale and could not simulate infiltration-excess runoff, which may be important at the subdaily or hourly scale [*Dingman*, 2008]. Both models also do not explicitly simulate the groundwater dynamics, which for our study area is a reasonable assumption as the groundwater table is usually much deeper than crop roots in this area [*Fan et al*., 2013]; there is no major aquifer system in West Africa [*Taylor et al*., 2012b], and few pumping irrigation systems have been adopted for low-value sorghum production [*MacDonald et al*., 2012]. Different parameterizations of hydrological processes may lead to inconsistent results, and thus, we recommend that future studies evaluate these types of effects in semiarid environments like West Africa.

The effect of a 10% delay of rainy season (Experiment (3)) is a yield loss for all cultivars, but whether modern or traditional varieties are more susceptible is less clear, due to the different parameterizations for photoperiod sensitivity in the two models. Because that SARRA-H only uses one photoperiodic variety in West Africa while APSIM adopts a latitude-dependent photoperiod parameterization, we are more confident in the APSIM-simulated yield responses to the delay of rainy season: a relatively small response for the modern cultivar due to its weak photoperiod sensitivity but a significant yield decrease (i.e., −10%) for the traditional cultivar due to elevated water stress at the end of rainy season. This yield change in most dry sites is similar in magnitude to yield changes caused by ±10% change in other rainfall characteristics (i.e., rainfall frequency, intensity, and length). This demonstrates that rainy season delay, or rainy season phase shifts, in general, may have a non-negligible impact on crop yield. When combining this change with a warming temperature (which shortens growth cycle), a delayed rainy season may result in a more complex change [*Sultan et al*., 2014] (also see Figure S9 in the supporting information).

5. Conclusion

Our study provides a comprehensive assessment of how different seasonal-scale rainfall characteristics affect sorghum yields in West Africa, by combining a new synthetic rainfall model and two independently validated crop models. Overall, our results support the idea that the influence of rainfall on crop yield is primarily dictated by the total rainfall amount during the rainy season. However, dry regions also have a large sensitivity to specific intraseasonal rainfall characteristics, with more drizzle (i.e., more frequent but less intense rainfall) leading to a yield loss. Only when MAP is higher than 600 mm/yr (for APSIM and 500 mm/yr for SARRA-H) does more frequent rainfall bring benefits to crop yield. A delayed rainy season, in general, leads to a yield loss for most dry sites in West Africa. Overall, we believe that our results have important implications for the design of future climate impact studies for rainfed agriculture and also provide information relevant for designing specific crop adaptations in West Africa.

Acknowledgments
This work has been funded by the U.S. National Science Foundation (SES-1048946), the Rockefeller Foundation, French National Research Agency (ANR) through the ESCAPE project (ANR-10-CEPL-005), and the France-Stanford Center for Interdisciplinary Studies. All the data in this study can be requested from Kaiyu Guan (kaiyug@stanford.edu) and David Lobell (dlobell@stanford.edu). We acknowledge the World Climate Research Programme's Working Group on Coupled Modelling, which is responsible for CMIP, and we thank the climate modeling groups for producing and making available their model output.

The Editor thanks two anonymous reviewers for their assistance in evaluating this paper.

Appendix A

The 16 models used in Figure 1 are the following: CCSM4, CMCC-CMS, CNRM-CM5, CSIRO-Mk3-6-0, GFDL-CM3, GFDL-ESM2G, GFDL-ESM2M, IPSL-CM5A-LR, IPSL-CM5A-MR, IPSL-CM5B-LR, MIROC5, MPI-ESM-LR, MPI-ESM-MR, MRI-CGCM3, NorESM1-M, and bcc-csm1-1.

References

Alagarswamy, G., D. Reddy, and G. Swaminathan (1998), Durations of the photoperiod-sensitive and -insensitive phases of time to panicle initiation in sorghum, *Field Crop. Res.*, *55*, 1–10.

Baron, C., B. Sultan, M. Balme, B. Sarr, S. Traore, T. Lebel, S. Janicot, and M. Dingkuhn (2005), From GCM grid cell to agricultural plot: Scale issues affecting modelling of climate impact, *Philos. Trans. R. Soc. London B. Biol. Sci.*, *360*(1463), 2095–2108, doi:10.1098/rstb.2005.1741.

Berg, A., B. Sultan, and N. de Noblet-Ducoudré (2010), What are the dominant features of rainfall leading to realistic large-scale crop yield simulations in West Africa?, *Geophys. Res. Lett.*, *37*, L05405, doi:10.1029/2009GL041923.

Biasutti, M. (2013), Forced Sahel rainfall trends in the CMIP5 archive, *J. Geophys. Res. Atmos.*, *118*, 1613–1623, doi:10.1002/jgrd.50206.

Biasutti, M., and A. H. Sobel (2009), Delayed Sahel rainfall and global seasonal cycle in a warmer climate, *Geophys. Res. Lett.*, *36*, L23707, doi:10.1029/2009GL041303.

Crétat, J., E. K. Vizy, and K. H. Cook (2013), How well are daily intense rainfall events captured by current climate models over Africa?, *Clim. Dyn.*, *42*(9–10), 2691–2711, doi:10.1007/s00382-013-1796-7.

Dingkuhn, M., M. Kouressy, M. Vaksmann, B. Clerget, and J. Chantereau (2008), A model of sorghum photoperiodism using the concept of threshold-lowering during prolonged appetence, *Eur. J. Agron.*, *28*(2), 74–89, doi:10.1016/j.eja.2007.05.005.

Dingman, L. (2008), *Physical Hydrology*, Waveland Press Inc, Long Grove, IL.

Fan, Y., H. Li, and G. Miguez-Macho (2013), Global patterns of groundwater table depth, *Science*, *339*(6122), 940–943, doi:10.1126/science.1229881.

Glotter, M., J. Elliott, D. McInerney, N. Best, I. Foster, and E. J. Moyer (2014), Evaluating the utility of dynamical downscaling in agricultural impacts projections, *Proc. Natl. Acad. Sci. U.S.A.*, *111*(24), 8776–8781, doi:10.1073/pnas.1314787111.

Good, S. P., and K. K. Caylor (2011), Climatological determinants of woody cover in Africa, *Proc. Natl. Acad. Sci. U.S.A.*, *108*(12), 4902–4907, doi:10.1073/pnas.1013100108.

Guan, K., S. P. Good, K. K. Caylor, H. Sato, E. F. Wood, and H. Li (2014a), Continental-scale impacts of intra-seasonal rainfall variability on simulated ecosystem responses in Africa, *Biogeosciences*, *11*(23), 6939–6954, doi:10.5194/bg-11-6939-2014.

Guan, K., E. F. Wood, D. Medvigy, J. Kimball, M. Pan, K. K. Caylor, J. Sheffield, X. Xu, and M. O. Jones (2014b), Terrestrial hydrological controls on land surface phenology of African savannas and woodlands, *J. Geophys. Res. Biogeosci.*, *119*, 1652–1669, doi:10.1002/2013JG002572.

Hammer, G. L., E. van Oosterom, G. McLean, S. C. Chapman, I. Broad, P. Harland, and R. C. Muchow (2010), Adapting APSIM to model the physiology and genetics of complex adaptive traits in field crops, *J. Exp. Bot.*, *61*(8), 2185–2202, doi:10.1093/jxb/erq095.

Kouressy, M., M. Dingkuhn, M. Vaksmann, and A. B. Heinemann (2008), Adaptation to diverse semi-arid environments of sorghum genotypes having different plant type and sensitivity to photoperiod, *Agric. For. Meteorol.*, *148*(3), 357–371, doi:10.1016/j.agrformet.2007.09.009.

Kumar, S. R., G. L. Hammer, I. Broad, P. Harland, and G. McLean (2009), Modelling environmental effects on phenology and canopy development of diverse sorghum genotypes, *Field Crop. Res.*, *111*(1–2), 157–165, doi:10.1016/j.fcr.2008.11.010.

Lodoun, T., A. Giannini, P. S. Traoré, L. Somé, M. Sanon, M. Vaksmann, and J. M. Rasolodimby (2013), Changes in seasonal descriptors of precipitation in Burkina Faso associated with late 20th century drought and recovery in West Africa, *Environ. Dev.*, *5*, 96–108, doi:10.1016/j.envdev.2012.11.010.

MacDonald, A. M., H. C. Bonsor, B. É. Ó. Dochartaigh, and R. G. Taylor (2012), Quantitative maps of groundwater resources in Africa, *Environ. Res. Lett.*, *7*(2024009), doi:10.1088/1748-9326/7/2/024009.

Major, D. (1980), Photoperiod response characteristics controlling flowering of nine crop species, *Can. J. Plant Sci.*, *60*(3), 777–784, doi:10.4141/cjps80-115.

Markham, C. G. (1970), Seasonality of precipitation in the United States, *Ann. Assoc. Am. Geogr.*, *60*(3), 593–597.

Monerie, P.-A., B. Fontaine, and P. Roucou (2012), Expected future changes in the African monsoon between 2030 and 2070 using some CMIP3 and CMIP5 models under a medium-low RCP scenario, *J. Geophys. Res.*, *117*, D16111, doi:10.1029/2012JD017510.

Panthou, G., T. Vischel, and T. Lebel (2014), Recent trends in the regime of extreme rainfall in the Central Sahel, *Int. J. Climatol.*, *34*(15), 3998–4006, doi:10.1002/joc.3984.

Porporato, A., E. Daly, and I. Rodriguez-Iturbe (2004), Soil water balance and ecosystem response to climate change, *Am. Nat.*, *164*(5), 625–632, doi:10.1086/424970.

Ramarohetra, J., B. Sultan, C. Baron, T. Gaiser, and M. Gosset (2013), How satellite rainfall estimate errors may impact rainfed cereal yield simulation in West Africa, *Agric. For. Meteorol.*, *180*, 118–131, doi:10.1016/j.agrformet.2013.05.010.

Rodriguez-Iturbe, I., A. Porporato, L. Ridolfi, V. Isham, and D. R. Cox (1999), Probabilistic modelling of water balance at a point: The role of climate, soil and vegetation, *Proc. R. Soc. A*, *455*, 3789–3805.

Ruane, A. C., S. McDermid, C. Rosenzweig, G. A. Baigorria, J. W. Jones, C. C. Romero, and L. Dewayne Cecil (2014), Carbon-temperature-water change analysis for peanut production under climate change: A prototype for the AgMIP Coordinated Climate-Crop Modeling Project (C3MP), *Global Change Biol.*, *20*, 394–407, doi:10.1111/gcb.12412.

Sivakumar, M. (1992), Empirical analysis of dry spells for agricultural applications in West Africa, *J. Clim.*, *5*, 532–539.

Sultan, B., P. Roudier, P. Quirion, A. Alhassane, B. Muller, M. Dingkuhn, P. Ciais, M. Guimberteau, S. Traore, and C. Baron (2013), Assessing climate change impacts on sorghum and millet yields in the Sudanian and Sahelian savannas of West Africa, *Environ. Res. Lett.*, *8*(1014040), doi:10.1088/1748-9326/8/1/014040.

Sultan, B., K. Guan, M. Kouressy, M. Biasutti, C. Piani, G. L. Hammer, G. McLean, and D. B. Lobell (2014), Robust features of future climate change impacts on sorghum yields in West Africa, *Environ. Res. Lett.*, *9*(10104006), doi:10.1088/1748-9326/9/10/104006.

Taylor, K. E., R. J. Stouffer, and G. A. Meehl (2012a), An overview of CMIP5 and the experiment design, *Bull. Am. Meteorol. Soc.*, *93*(4), 485–498, doi:10.1175/BAMS-D-11-00094.1.

Taylor, R. G., et al. (2012b), Ground water and climate change, *Nat. Clim. Change*, *3*(4), 322–329, doi:10.1038/nclimate1744.

Thomey, M. L., S. L. Collins, R. Vargas, J. E. Johnson, R. F. Brown, D. O. Natvig, and M. T. Friggens (2011), Effect of precipitation variability on net primary production and soil respiration in a Chihuahuan Desert grassland, *Global Change Biol.*, *17*(4), 1505–1515, doi:10.1111/j.1365-2486.2010.02363.x.

Traoré, S. B., et al. (2011), Characterizing and modeling the diversity of cropping situations under climatic constraints in West Africa, *Atmos. Sci. Lett.*, *12*(1), 89–95, doi:10.1002/asl.295.